Progress In Electromagnetics Research B, Vol. 43, 19–33, 2012

AN IMAGE CORRECTION METHOD BASED ON ELECTROMAGNETIC SIMULATION FOR MICROWAVE INDUCED THERMO-ACOUSTIC TOMOGRAPHY SYSTEM

J. Song[1], Z. Q. Zhao[1, *], J. G. Wang[1], X. Z. Zhu[1], J. N. Wu[1], Y. L. Liu[1], and Q. H. Liu[2]

[1]School of Electronic Engineering, University of Electronic Science and Technology of China, Chengdu, Sichuan 611731, China

[2]Department of Electrical and Computer Engineering, Duke University, Durham, NC 27708, USA

Abstract—In microwave induced thermo-acoustic tomography (MITAT) system, radiation of an antenna is a near field problem which gives rise to a non-uniform distribution of microwave radiation power in detection area. Due to this non-uniform distribution, the contrast of MITAT image which is proportional to the absorbed microwave energy will not reflect the real characteristics (dielectric properties) of biological tissues. In this paper, an image correction method based on electromagnetic simulation is proposed to correct the image contrast affected by the non-uniform microwave radiation distribution. First, the distribution of the microwave radiation power is simulated through a numerical simulation framework. Conventional time-reversal mirror (TRM) technique is applied to reconstruct the image. Then the microwave power distribution is applied to correct the image. The method is numerically demonstrated. The two samples with the same microwave absorption property and with different microwave absorption properties are experimentally investigated. Both numerical simulations and experimental results demonstrate the good performance of the proposed method.

1. INTRODUCTION

Breast cancer is the most common female malignancy and the second leading cause of cancer mortality for women. Early diagnosis is

Received 2 July 2012, Accepted 30 July 2012, Scheduled 6 August 2012

* Corresponding author: Zhiqin Zhao (zqzhao@uestc.edu.cn).

the key to surviving breast cancer [1]. Microwave induced thermo-acoustic tomography (MITAT) has recently received more and more attentions with its great potential in early breast tumors detection [2–6]. Because it combines the advantages of microwave imaging [7] and ultrasound tomography. In MITAT system, a tissue is illuminated by an electromagnetic wave. Then the microwave energy absorbed by the tissue causes thermo-elastic expansion, which generates acoustic waves, termed thermo-acoustic waves. A tomographic image which represents the tissue microwave absorption properties is reconstructed from the recorded thermo-acoustic signals. Such image reflects the physiological and pathological status of the tissue because it has a high contrast of the electromagnetic radiation absorption rate between tumors and normal tissues [1–7].

Several thermo-acoustic image methods have been proposed in [8–13]. Chen et al. [8–10] exploited time reversal mirror (TRM) technique as a reconstruction algorithm in MITAT system. TRM technique is an efficient method with high spatial resolution and noise rejection features. Zeng et al. [11] presented a modified filtered back projection algorithm with combination wavelet to reconstruct the image. In order to compensate signal propagation attenuation in a tissue, gain compensation method was proposed by Geng and Wang [3]. All these papers assumed a uniform electromagnetic radiation (microwave source). The gray levels of the final MITAT image directly reflect the electromagnetic characteristics of illuminated biological tissues.

In real engineering, the specimen is placed at the near field zone of the antenna according to the wavelength and the size of the antenna. Near field radiation always gives rise to a non-uniform microwave power distribution [14, 15]. Therefore the absorbed microwave energy will not reflect the microwave absorption characteristic of a biological tissue. For example, though the energy absorption rate of a tumor is higher than that of normal tissues, the tumor may absorb less electromagnetic energy than the normal tissues if the tumor is put into the weak electromagnetic radiation area. This situation will result in serious consequences, such as missed detection or false alarm.

Aiming to solve the mentioned problem, an image correction method is proposed in this paper. The main idea of the method is to correct the MITAT image according to the simulated radiation power distribution. It is consisted of two steps. First, the distribution of the electromagnetic radiation is numerically simulated. Then, the image of the tissue absorption properties is reconstructed by using TRM technique, where the microwave radiation distribution is taken into consideration in the reconstruction procedure. In this procedure, the influence caused by non-uniform radiation can be effectively relieved

and the mapping relationship between image contrast and tissue electromagnetic parameter is accurately established.

The remainder of the paper is organized as follows. In Section 2, an image correction method is proposed. Its mechanism is analyzed and validated by some numerical simulations. Some experimental results are given in Section 3. Good performance of the method is demonstrated. Conclusions are drawn in the final section.

2. IMAGE CORRECTION METHOD

2.1. Mechanism of the Image in MITAT

For MITAT, the reconstructed image is related with the thermo-acoustic signals emitted from different tissues. The magnitude of the thermo-acoustic signal is proportional to the absorbed microwave energy. The relationship between the absorbed microwave energy and the thermo-acoustic signal can be expressed as [16]

$$p(t) = \frac{\beta}{4\pi C_V} \iiint \frac{\partial H(\vec{r}', t)}{\partial t} \frac{d\vec{r}'}{|\vec{r} - \vec{r}'|}, \tag{1}$$

where $p(t)$ is the waveform of the acoustic signal in specific location $\vec{r}$, $\vec{r}'$ is the source position vector, β is the coefficient of volume thermal expansion, C_V is the material specific heat capacity and $H(\vec{r}', t)$ is the heating function. The heating function can be approximated as

$$\frac{\partial H(\vec{r}', t)}{\partial t} \approx H(\vec{r}') \frac{\partial H(t)}{\partial t}, \tag{2}$$

with product separated contribution of the spatial $H(\vec{r}')$ and temporal $H(t) \approx \delta t$ parts. The heating function is then described as a deposition of microwave radiation power in the sample [16]:

$$H(\vec{r}') = \int_v \frac{\sigma}{2} \left|\vec{E}\right|^2 dv + \int_v \frac{\omega \varepsilon''}{2} \left|\vec{E}\right|^2 dv = p_{cond} + p_{el}, \tag{3}$$

taking into account the conductivity losses p_{cond} and the dielectric losses p_{el}. σ is the conductivity, $\vec{E}$ is the electrical field, ω is the angular frequency and ε'' is the imaginary part of the permittivity. According to (1)–(3), the intrinsic contrast in thermo-acoustic image is dominated by electric loss in the tissue. Thus, samples with high conductivity exhibit higher energy absorption than tissues with lower conductivity. Therefore, the resulting thermo-acoustic image maps dielectric parameters distribution of the imaged object [16].

In [3], the microwave absorption property of tissue is summarized as the absorption coefficient,

$$\alpha=\omega\sqrt{\frac{\mu\varepsilon}{2}\left[\sqrt{1+\left(\frac{\sigma}{\omega\varepsilon}\right)^2}-1\right]}, \tag{4}$$

where ω is the angular frequency, μ the permeability, ε the permittivity, and σ the conductivity. The complex dielectric property of the tissue determines the propagation and absorption features of microwave. Also it can be found that the induced thermo-acoustic pressure depends on the microwave intensity and the complex dielectric constant of the tissue samples. Thus the thermo-acoustic signals can reflect the tissue characteristic when the microwave intensity was relative uniform.

Time-reversal mirror (TRM) technique is applied as image reconstruction method by using the thermo-acoustic signals $p(t)$ due to its advantage in MITAT image [8–10]. The procedure of TRM can be expressed as

$$I(\vec{r},t)=\sum_{s=1}^{M}\int_{-\infty}^{+\infty}\bar{p}_s(\omega)\sum_{k=1}^{K}G_c(\vec{r}_k,\,\vec{r},\,\omega)\bar{G}_s(\vec{r}_k,\,\vec{r}_s,\,\omega)e^{-j\omega t}d\omega, \tag{5}$$

$$p_s(\omega)=\int_{-\infty}^{+\infty}p(t)e^{-j\omega t}dt, \tag{6}$$

where $I(\vec{r},t)$ is the pixel value at location $\vec{r}$ in imaging zone at moment t, M the totality of thermo-acoustic signals, K the totality of sensors, G_c a Green's function from the sensor to field location $\vec{r}$, and $\bar{G}_s$ a conjugate Green's function from acoustic source to the sensor.

The relationship between pixel values and thermo-acoustic signals is established through the TRM reconstruction procedure. According to (1)–(4), the thermo-acoustic signal is related with the absorbed microwave energy. The mapping relationship between the pixel value and absorbed microwave energy can be expressed as

$$I\propto p(t)\propto H. \tag{7}$$

In previous literatures [1–4], the microwave radiation power is considered as a constant within a tomographic plane. However, in real situation, due to the radiation of antenna and the surrounding environment, it is impossible to achieve a perfect uniform distribution of radiation power in an imaging plane. This means that the $\vec{E}$ in Eq. (3) is not a constant. Therefore, the magnitude of thermo-acoustic signal will be affected not only by the electrical parameters of the tissue, but also by the non-uniform distribution of electrical fields. The reconstructed image using the thermo-acoustic signal will not reflect the real tissue electromagnetic property.

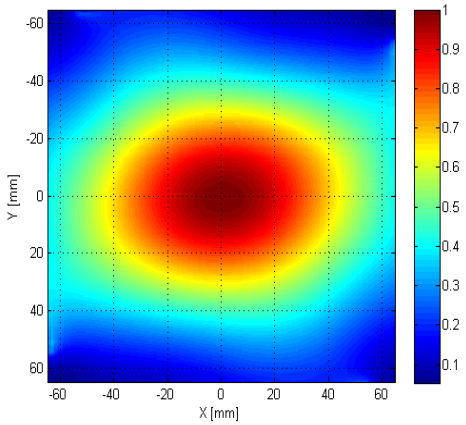

Figure 1. Simulated radiation power distribution in tomography plane.

2.2. The Effects of Radiation Power Distribution

In order to illustrate the effects of the radiation power distribution on the MITAT image, some numerical simulations have been done. A simulation framework has been established. In the framework, finite integration time domain (FITD) is used to simulate the microwave radiation power distribution [16]. Pseudo-spectral time domain (PSTD) method is applied to simulate the acoustic wave propagation and to reconstruct the image [17–20].

In the simulation of the microwave radiation power distribution, microwave horn antenna, scanning bowl, ultrasound coupling medium and ultrasonic transducers are all taken into accounted in order to get a more realistic simulation. The simulated power distribution of one cross section along z-direction is shown in Fig. 1. In order to illustrate the problem, the figure has been normalized. Obviously the radiation power is non-uniformly distributed, which gradually decays from the center to the edge. At the edge of the radiation zone (for example 40 mm away from the center), the radiation power is only about a half of that at the center. This implies that if a tumor is placed at the edge of the illumination area, it receives less microwave energy than it is placed at the center of the area. Naturally the pixel value mapped by less absorbed microwave energy will be smaller. The real tissue electromagnetic properties are not accurately reflected by the reconstructed image. This phenomenon will be verified in the following numerical simulations.

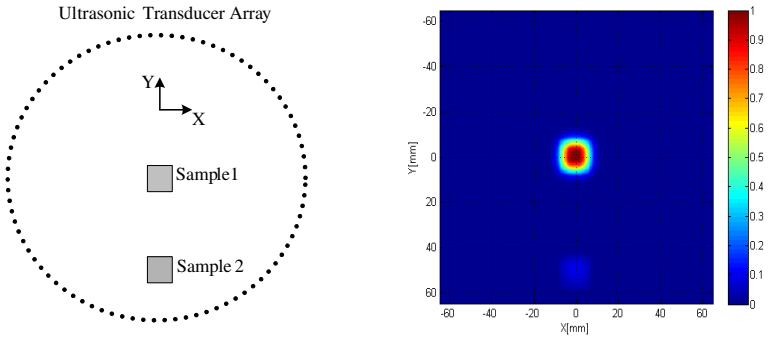

Figure 2. Simulation result: (a) The sketch of simulation setup; (b) Reconstructed image using conventional TRM technique.

Two samples with same electromagnetic parameters are simulated. Their sizes are both 15 mm × 15 mm. The centers of the targets are set at (0, 0) and (0, 52.5), respectively. Sample 1 is placed at the center of the scanning container, the other one is placed at the edge of the scanning container. Ultrasonic transducer array is around the samples. The simulation setup is shown in Fig. 2(a). The processes including microwave radiation, thermal acoustic wave propagation and image reconstruction are numerically simulated. Fig. 2(b) is the image reconstructed by using the conventional TRM technique.

From Fig. 2(b), it shows that the intensity of sample 2 is not as strong as that of sample 1 though they have the same electromagnetic property. The reason is that the electrical field of microwave radiation at the edge of the scanning bowl is much weaker than that at the center. According to (1)–(3), the thermo-acoustic signals generated by sample 2 are therefore much smaller than that of sample 1. The smaller thermo-acoustic signals induce the smaller intensity values in the image. Through this simulation, we can conclude that the non-uniform distribution of the radiation power will distort the relationship between the tissue property and the contrast of the image.

2.3. Correction Method

Aiming to solve the problem brought by non-uniform distribution of radiation power as demonstrated in the previous sub-section, an image correction method is proposed. Similar method is used in [20]. The photo-acoustic image is normalized by the light distribution in the object. The main steps of this method are summarized as follow:

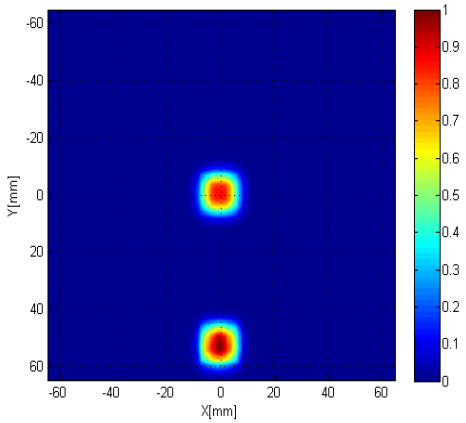

Figure 3. The reconstructed image with the proposed correction method.

1) Reconstruct the image through the TRM technique. This is the same as the conventional TRM.
2) Simulate the distribution of microwave radiation power through the system simulation framework.
3) Relieve the effect of non-uniform radiation power distribution from the reconstructed image by step 1). The mapping relationship between the pixel and absorbed microwave energy is modified as

$$I'(\vec{r}) = I(\vec{r})/H(\vec{r}), \tag{8}$$

where $I'(\vec{r})$ is pixel value obtained by the correction method at location $\vec{r}$, $I(\vec{r})$ the pixel value obtained by conventional method, and $H(\vec{r})$ the heating function.

In order to validate the effectiveness of the proposed correction method, same simulation data as in Section 2.2 has been used. Fig. 3 is the result by using the proposed correction method. Obviously, the strength of sample 2 is highly enhanced in the image. The amplitudes of the two samples are almost the same. This means that the effect induced by the non-uniform distribution is well relieved by using this correction method. This will be further demonstrated through some experiments. It is necessary to state that the intensity at the power distribution edge is very small and may induce the value of new pixel intensity being astronomically high. The noise is filtered to avoid this situation.

Figure 4. Circular scanning thermo-acoustic tomography system.

3. EXPERIMENTAL RESULTS

We have established a circular scanning system which is applied to receive the thermo-acoustic signals. In this way, one can obtain significant signal to noise ratio (SNR) compared with a linear array [21, 22]. The picture of circular scanning system is shown in Fig. 4. The z axis is perpendicular to the aperture plane of the horn antenna. The x axis is perpendicular to the drawing plane and points outward. The y axis is in the drawing plane pointing to the right. A 2.45 GHz microwave generator transmits microwave pulses toward the specimen. The pulse duration time is 0.5 µs in the experiments. The peak power of a single microwave pulse is set to 3 kW. A rectangle pulse modulator is employed to trigger the microwave generator and to control the pulse repetition rate. Microwave energy is delivered to a microwave antenna through a standard rectangular waveguide. The microwave antenna is a circular horn whose diameter is 15 cm. It is designed to radiate the microwave as equally as possible to heat the sample.

The specimen is placed in a teflon container, which is fixed onto a two-dimensional x-y scanning plane. The distance between the imaged specimen and microwave antenna is about 6.65 cm. A computer controls the motor to drive the scanning device. Four transducers (V314-SU, OLYMPUS) amounted on the container wall rotate around the sample. Thermo-acoustic signals are sampled at different angles. The central frequency of the ultrasonic transducer is 1 MHz. The piezoelectric output of the ultrasonic transducer is connected to a pulse amplifier. The amplified acoustic signals are acquired by a data acquisition card (PCI-1714, ADVANTECH) through the un-focused

ultrasonic transducers.

Based on the experimental system, a series of simplified experiments are performed to verify the correction method. An experiment of two targets with same dielectric property is carried out. Phantom targets are made from agar, salt and water et al.. The relative permittivity and conductivity of phantom are about 60 and 5 S/m. This kind of phantom has similar electromagnetic parameters as tumor whose relative permittivity and conductivity are 50 and 4 S/m, respectively. Another experiment is two samples (fat and phantom) with different microwave absorption properties. The relative permittivity and conductivity of fat are 5.5 and 0.4 S/m. The fat exhibits lower microwave absorption than that of the phantom.

In reality, the biological tissue is heterogeneous and the heterogeneity will affect the energy distribution. But we can predict the tissue model, and obtain a coarse energy distribution. It will still give some improvements compared with the condition without doing any modifications.

3.1. Experimental Results for Two Targets with the Same Electromagnetic Parameters

In this experiment, one target is placed at the center of scanning bowl and the other one is placed at the edge. Figs. 5(a) and (b) show the picture of the phantoms and the sketch of experiment setup, respectively. Fig. 5(c) is the result by using the conventional TRM. Fig. 5(d) shows the result by using the proposed correction method. Figs. 5(e) and (f) are amplitudes of the cross sections plots along y-direction.

The goal of the MITAT is to discriminate the electromagnetic properties for different tissues according to the contrast of the image [23–27]. Ideally, the samples with the same electromagnetic parameters should have the same pixel intensity in the image. However, Fig. 5(c) shows that the sample placed at the radiation zone edge has much smaller intensity than that of the sample at the center. This result indicates that the microwave absorption properties of samples are not accurately reflected due to the non-uniform distribution of microwave radiation. In Fig. 5(d), the pixel intensity values of the two samples are almost the same. The effect of the non-uniform distribution of microwave radiation is relieved by the proposed correction method.

Similarity S is used to describe the reconstruction performances. It is defined as

$$S = P_{2\max}/P_{1\max}, \tag{9}$$

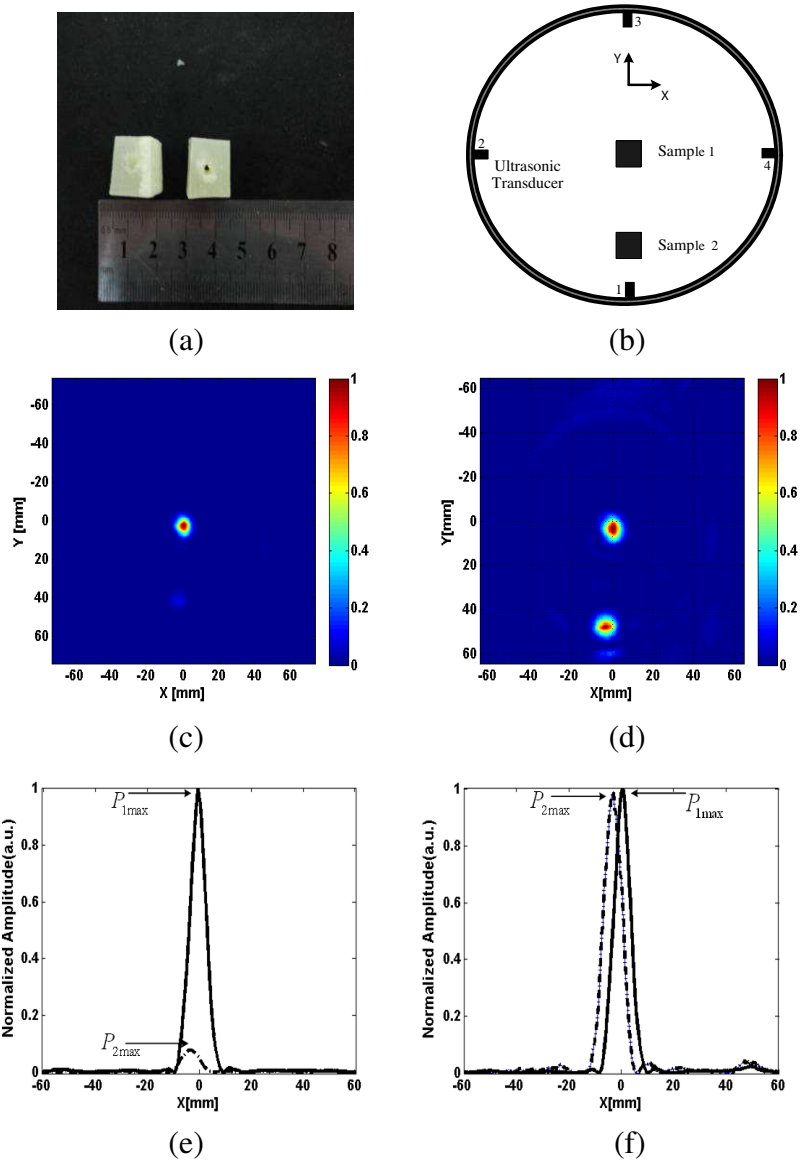

Figure 5. Actual picture, experiment setup and reconstructed images. (a) Optical photo of phantoms; (b) The sketch of experiment setup; (c) Reconstructed image using conventional TRM; (d) Reconstructed image using the proposed correction method; (e) Reconstructed image using conventional TRM ($S = 0.1$); (f) Reconstructed image using the proposed correction method ($S = 0.97$).

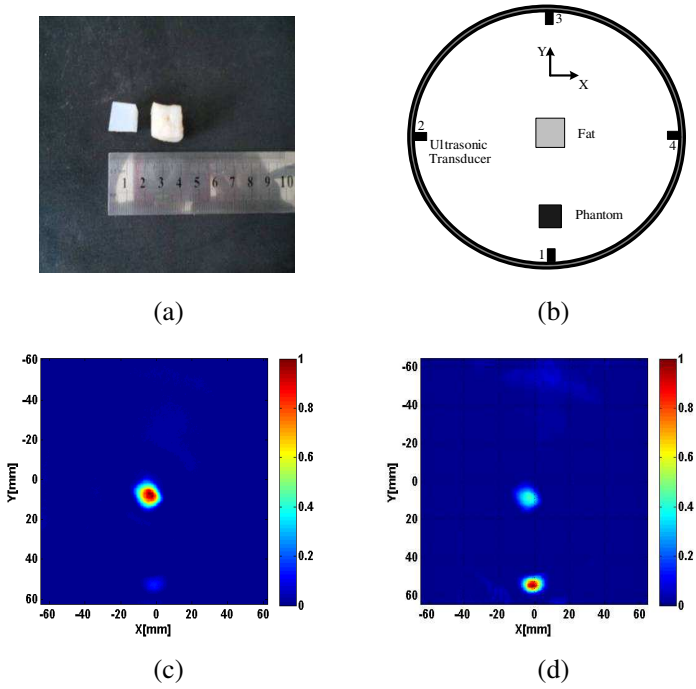

Figure 6. Actual picture, experiment setup and reconstructed image. (a) Optical photo of targets; (b) The sketch of experiment setup; (c) Reconstructed image using conventional TRM; (d) Reconstructed image using the proposed correction method.

where $P_{2\max}$ is the peak value of sample 2 and $P_{1\max}$ the peak value of sample 1. The peak values mapped by two samples with the same microwave absorption property should be equal, i.e., $S = 1$.

The amplitudes of the cross sections along y-direction are plotted in Figs. 5(e) and (f). From Fig. 5(e), the S obtained by conventional TRM is 0.1, while the similarity is 0.97 after using the correction method. This indicates that the electromagnetic properties of the samples are better reflected by the image modified by the correction method.

3.2. Experimental Results for Two Targets with Different Electromagnetic Parameters

The method is further studied through an experiment for two targets (fat and phantom) with different electromagnetic parameters. The fat which has a less microwave absorption rate is placed at the center

where the radiation power is stronger. The phantom which has a larger microwave absorption rate is placed at the edge of the container. Fig. 6(a) shows the picture of samples and Fig. 6(b) is the sketch of experiment setup. Figs. 6(c) and (d) are the results obtained by conventional TRM method and the proposed method, respectively.

In Fig. 6(c), the pixel intensity of the phantom is much smaller than that of the fat. In theory, the thermo-acoustic excited from the fat should have smaller amplitude because of its less microwave absorption. Therefore, the pixel intensity of the fat is much smaller than that of the phantom in the reconstructed image. However, in Fig. 6(c), this law is not reflected due to the non-uniform distribution of microwave radiation.

Figure 6(d) is the result by using the proposed correction method. It can be found that the contrast of the image accurately reflects the microwave absorption property of tissue. Specific absorption rate (SAR) is used to measure the microwave absorption in general [12]. According to [19], the ratio of the SARs between tumor and fat is about $9 \sim 20$. In Fig. 6(c), the ratio of the SARs between the phantom and the fat is only 0.22, which is far away from that of [19]. But from Fig. 6(d), the ratio is 10.92, which is at the interval mentioned by [19]. Such image can reflect the physiological and pathological status of the tissue in a certain extent because it reflects the different microwave absorption properties between tumor and normal tissue.

4. CONCLUSIONS

The purpose of MITAT system is to reflect the microwave absorption property of a tumor through the contrast of the image. However, in real engineering, due to the non-uniform distribution of microwave radiation power, the image contrast often does not reflect the microwave absorption properties of tissue accurately. Aiming to solve this problem, an image correction method is proposed in this paper. The fundamental of the method is to correct the image by using the numerically calculated microwave radiation power distribution. The effect to the image quality caused by this non-uniform distribution is relieved based on the distribution. Both numerical and experimental results demonstrate the effectiveness of the proposed correction method.

ACKNOWLEDGMENT

This research is supported by NSFC (No. 60927002).

REFERENCES

1. Guo, B., J. Li, H. Zmuda, and M. Sheplak, "Multifrequency microwave-induced thermal acoustic imaging for breast cancer detection," *IEEE Trans. Biomed. Eng.*, Vol. 54, No. 11, 2000–2010, 2007.
2. Ku, G., B. D. Fornage, X. Jin, M. Xu, K. K. Hunt, and L. V. Wang, "Thermo-acoustic and photo-acoustic tomography of thick biological tissues toward breast imaging," *Technol. Cancer Res. Treat.*, Vol. 4, 1–7, 2005.
3. Geng, K. and L. V. Wang, "Scanning microwave-induced thermo-acoustic tomography: Signal, resolution, and contrast," *Med. Phys*, Vol. 28, No. 1, 4–10, 2001.
4. Nie, L. M., D. Xing, Q. Zhou, D. W. Yang, and H. Guo, "Signal processing in scanning thermoacoustic tomography in biological tissues," *Med. Phys.*, Vol. 35, No. 9, 4026–4032, 2008.
5. Xu, Y. and L. V. Wang, "Microwave-induced thermo-acoustic scanning CT for high-contrast and noninvasive breast cancer imaging," *Med. Phys.*, Vol. 28, 1519–1524, 2001.
6. Feng, D., Y. Xu, G. Ku, and L. V. Wang, "Microwave-induced thermo-acoustic tomography: Reconstruction by synthetic aperture," *Med. Phys.*, Vol. 28, 2427–2431, 2001.
7. Catapano, I., L. Di Donato, L. Crocco, O. M. Bucci, A. F. Morabito, T. Isernia, and R. Massa, "On quantitative microwave tomography of female breast," *Progress In Electromagnetics Research*, Vol. 97, 75–93, 2009.
8. Chen, G. P., Z. Q. Zhao, W. J. Zheng, Z. P. Nie, and Q. H. Liu, "Application of time reversal mirror technique in microwave-induced thermo-acoustic tomography system," *Science in China Series E: Technological Science*, Vol. 52, No. 7, 2087–2095, 2009.
9. Chen, G. P., Z. Q. Zhao, Z. P. Nie, and Q. H. Liu, "A computational study of time reversal mirror technique for microwave-induced thermo-acoustic tomography," *Journal of Electromagnetic Waves and Applications*, Vol. 22, No. 12, 2191–2204, 2008.
10. Chen, G. P., W. B. Yu, Z. Q. Zhao, Z. P. Nie, and Q. H. Liu, "The prototype of microwave-induced thermo-acoustic tomography imaging by time reversal mirror," *Journal of Electromagnetic Waves and Applications*, Vol. 22, No. 11, 1565–1574, 2008.
11. Zeng, L., D. Xing, H. Gu, D. Yang, S. Yang, and L. Xiang, "High anti-noise photo-acoustic tomography based on a modified filtered back projection algorithm with combination wavelet," *Med. Phys.*,

Vol. 34, 556–563, 2007.

12. Xie, Y., B. Guo, J. Li, G. Ku, and L. V. Wang, "Adaptive and robust methods of reconstruction (ARMOR) for thermo-acoustic tomography," *IEEE Trans. Biomed. Eng.*, Vol. 55, 2741–2752, 2008.
13. Xu, M. and L. V. Wang, "Time-domain reconstruction for thermo-acoustic tomography in a spherical geometry," *IEEE Trans. Med. Imag.*, Vol. 21, No. 7, 814–822, 2002.
14. Yan, W., J.-D. Xu, N.-J. Li, and W.-X. Tan, "A novel fast near-field electromagnetic imaging method for full rotation problem," *Progress In Electromagnetics Research*, Vol. 120, 387–401, 2011.
15. Qi, Y., W. Tan, Y. Wang, W. Hong, and Y. Wu, "3D bistatic Omega-K imaging algorithm for near range microwave imaging systems with bistatic planar scanning geometry," *Progress In Electromagnetics Research*, Vol. 121, 409–431, 2011.
16. Kellnberger, S., A. Hajiaboli, D. Razansky, and V. Ntziachristos, "Near-field theroacoustic tomography of small animals," *Phys. Med. Biol.*, Vol. 56, 3433–3444, 2011.
17. Liu, Q. H, "The pseudospectral time-domain (PSTD) algorithm for acoustic waves in absorptive media," *IEEE Trans. Ultrason., Freroelect., Freq. Contr.*, Vol. 45, No. 4, 1044–1055, 1998.
18. Treeby, B. E. and B. T. Cox, "k-wave: MATLAB toolbox for the simulation and reconstruction of photo-acoustic wave fields," *Journal of Biomedical Optics*, Vol. 15, No. 2, 021314, 2010.
19. Chen, G. P. and Z. P. Nie, "Critical technologies research of the microwave-induced thermo-acoustic tomography system," 17–19, Dissertation, University of Electronic Science and Technology of China, 2009.
20. Razansky, D., M. Distel, C. Vinegoni, and R. Ma, "Multispectral opto-acoustic tomography of deep-seated fluorescent proteins in vivo," *Nature Photonics*, Vol. 3, 412–417, 2009.
21. Nie, L. M., D. Xing, D. W. Yang, L. M. Zeng, and Q. Zhou, "Detection of foreign body using fast thermo-acoustic tomography with a multi-element linear transducer array," *Appl. Phys. Lett.*, Vol. 90, 174109–174111, 2007.
22. Yang, D. W., D. Xing, S. H. Yang, and L. Z. Xiang, "Fast full-view photo-acoustic imaging by combined scanning with a linear transducer array," *Opt. Express*, Vol. 15, 15566–15575, 2007.
23. Yuan, Z. and H. B. Jiang, "Quantitative photo-acoustic tomography: Recovery of optical absorption coefficient maps of heterogeneous media," *Appl. Phys. Lett.*, Vol. 88, 231101–231103,

2006.

24. Xu, Y. and L. V. Wang, "Reconstructions in limited-view thermo-acoustic tomography," *Med. Phys.*, Vol. 31, 724–733, 2004.
25. Lazebnik, M., "A large-scale study of the ultrawideband microwave dielectric properties of normal, benign and malignant breast tissues obtained from cancer surgeries," *Phys. Med. Biol.*, Vol. 52, 6093–6115, 2007.
26. Su, J. L. and J. C. Lin, "Thermoelastic signatures of tissue phantom absorption and thermal expansion," *IEEE Trans. Biomed. Eng.*, Vol. 43, 178–182, 1987.
27. Mashal, A., J. H. Booske, and S. C. Hagness, "Toward contrast-enhanced microwave-induced thermo-acoustic imaging of breast cancer: An experimental study of the effects of microbubbles on simple thermo-acoustic targets," *Phys. Med. Biol.*, Vol. 54, 641–650, 2009.